



Electron Microprobe Analysis of Minerals in Soil Aggregates

Azuma, Junzo

Nakamura, Toshihiro

Ishizawa, Shuichi

(Citation)

神戸大学農学部研究報告, 12(2):283-295

(Issue Date)

1977

(Resource Type)

departmental bulletin paper

(Version)

Version of Record

(JaLCD0I)

<https://doi.org/10.24546/00228543>

(URL)

<https://hdl.handle.net/20.500.14094/00228543>



ELECTRON MICROPROBE ANALYSIS OF MINERALS IN SOIL AGGREGATES

Junzo AZUMA*, Toshihiro NAKAMURA**, and Shuichi ISHIZAWA*

(Received for publication on August 10, 1976)

Abstract

With the object of discerning the arrangement of soil minerals composing soil aggregate, polished section specimens and unpolished sprinkling specimens of volcanic and nonvolcanic-ash soils were examined by electron microprobe analyzer. According to the gross difference of interelemental relationships in micro-area, the following Points were ascertained.

1. Soil aggregates consisting of various minerals.
2. Clay and oxides of iron and aluminum illuviated in layer on the surface of sand grain.
3. Skeleton grains and voids included within clay matrix, and mottled iron on the grains.
4. Clay and oxides, in general, playing an important role in cementing between grains as well as between aggregates.

As reported in the foregoing paper¹⁾, it was found that a scanning electron microscope is very useful for the study of the surface microstructure of soil aggregates. There are, however, many aspects to be studied on the condition of cementing materials between soil particles or of a plasma on the surface of skeleton grains.

CHILDS⁴⁾, BREWER²⁾, and GALLAHER^{6,7)} *et al.* used an electron microprobe analyzer to illustrate interelemental relationships in concretions or pans found in soils in relation to the process of their formation. Using such analyzer, SOMASIRI and HUANG¹²⁾ indicated the presence of more than one phase of feldspar in soil, and SAWHNEY¹⁰⁾ revealed that precipitated phosphates occurred mostly as complex compounds containing aluminum, iron, silicon, calcium, and phosphorus in the discrete phosphate grain of soils and sediments.

This paper is one of the results on electron microprobe analyses of the arrangement pattern of soil particles and their component minerals on the basis of elemental composition. This analyzer Permits us to perform quan-

titative as well as qualitative study of soils in micron-scale *in situ*.

Materials and Methods

Soils

The soils used in this study were two kinds of volcanic and nonvolcanic-ash soils. Selection of these soil were based on their differences in chemical and mineralogical composition as reported in the foregoing paper¹⁾. Water-stable aggregates prepared in laboratory (synthetic aggregate) as mentioned later were further used as a referential sample.

Preparation of synthetic aggregate

After kaolinite clay, quartz sand, glass beads, and colloidal iron were mixed under a slurry condition, this mixture was incubated in an oven maintained at 30°C over a period of 2 weeks, and then sieved in water. Water-stable aggregates remained on a wire sieve of 9 mesh were collected and used as a referential sample.

Preparation of specimens

Two kinds of specimen were used.

a) section specimen

Following moisture removal by exchanging

* Laboratory of Soil Science

** Shinmeito Co., Ltd.

with propylene oxide under a decreasing pressure, a few grains of soil were impregnated, according to LUFT's method⁹⁾, with a given mixture of EPON resin no. 812 (Shell Chemical Company), D.D.S.A. (dodecenyl succinic anhydride; hardner), M.N.A. (methyl nadic anhydride; hardner), and D.M.P.-30 (tridimethylaminomethyl phenol; accelerator) in a gelatin capsule vial. This resin is suitable for the impregnation and polish of small soil aggregates and is thermally stable under the electron beam^{3,8)}. Since the reaction of this resin is temperature dependent, the vials were placed in an oven maintained at 35°C and allowed to set for 24 hours. After that the temperature was raised in increment 13°C up to 61°C at 12-hour intervals. The resultant embedded soils, 0.5 cm in diameter and approximately 1 cm in height, were detached by breaking the gelatin vials. Although thin sections may be desirable for some microprobe analyses^{3,13)}, they were not required for this study. Rough grinding and polishing of the embedded soils were made on universal auto polisher (Wingo Co., Ltd.) with an abrasive slurry consisting of carborundum (25 μm in particle diameter) and kerosine. The final polishing was accomplished by successive use of inert chromic oxide⁵⁾ slurried in kerosine on a glass plate and a polishing felt cloth. The sections were washed with water and kerosine to remove a polishing material. Their polished surfaces were then coated with a thin film of carbon and gold using a vacuum method.

b) sprinkling specimen

Soil samples used for the study of elemental composition on their original surface were mounted in a different way from that in section specimen, because most of their original surface were removed off by the latter. According to a sprinkling method¹¹⁾, air dried soils were sprinkled immediately onto silver paste on the stub for the electron microprobe analyzer prior to carbon-and gold-coating.

Elemental analysis by electron microprobe analyzer

Elemental analysis of soils was made by using Shimadzu-ARL model EMX-SM (single

instrument combining the features of electron microprobe analyzer and scanning electron microscope). An acceleration voltage of 30 kV and a specimen current less than 0.01 μA were used for all samples. A lithium fluoride (LiF) crystal was used for the analyses of iron, manganese, potassium, and calcium, an ammonium dihydrogen phosphate (ADP) crystal for silicon and phosphorus, and a rubidium acid phtharate (RAP) crystal for aluminum, magnesium, and sodium. Pure metal standard was used for silicon, aluminum, iron, magnesium, and manganese, orthoclase for potassium, and apatite for calcium and phosphorus.

Use of this Shimadzu-ARL analyzer with the high take-off angle of 52.5° may be particularly reasonable to minimize irregular absorption effect produced by not enough smooth surface on the unpolished sprinkling specimen. A specimen current picture and a characteristic $K\alpha$ x-ray area-scanning image were recorded photographically from the oscilloscope screen. The instrumental exposure times and sensitivities were varied from element to element, and so the peak height of element in one figure is not comparable to that in another.

Result and Discussion

The electron microprobe analyzer made it possible to analyze component elements in

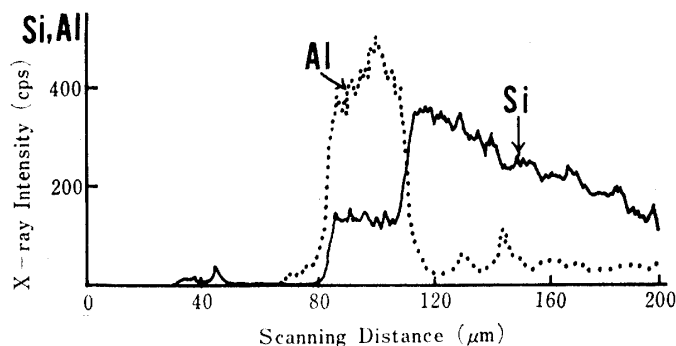


Fig. 1. Elemental distribution at the line (depicted in specimen current picture in Fig. 6) across a specimen of Fig. 6.

X-ray intensity was recorded as counts per second to determine the relative amounts of the elements at the line in the specimen.

small area on the surface of soil specimens. Electron beam scanning of selected area of the specimen produced an image of relative concentration of each element throughout the area. A line scanning curve, which corresponds to profiling of the x-ray intensity, displayed, as shown in Figs. 1, 2, 3, and 4, the variations of elemental composition to be compared in a given area of the specimen. From these results, the interelemental relationships may be established.

The x-ray images of silicon, aluminum, and iron and the congruent picture of specimen current of the section of synthetic aggregate prepared as a referential sample are given in Fig. 5 (A-D). Relative distribution of individual element is shown in the x-ray images, in which its semiquantitative estimation may be possible according to varying shades of white to black. Increasing lightness in the x-ray images corresponds to increasing concentration of the element concerned. A specimen current is sensitive to the variation in mean atomic number^{3,13} and its picture indicates essentially the variation in phase chemistry in relation to the morphology of specimen. The disposition of kaolinite clay is capable of detecting from the x-ray image of aluminum, because except the kaolinite clay aluminum was not contained in component materials of this aggregate. A codominance of aluminum and iron in the corresponding region may suggest that the kaolinite clay binds the colloidal iron together to make a massive matrix. There were resins surrounding the synthetic aggregate at the upper bright part of Fig. 5 (A). The concentration of silicon was high in the areas in which aluminum and iron were present in only minor proportions. Thus, the quartz sand appears to be connected with iron and kaolinite clay because of the distribution of iron and aluminum surrounding silicon.

Figure 6 is specimen current picture and the corresponding x-ray images of component element of a polished section specimen of Higashishiroyama soil. As shown in x-ray images of Fig. 6 (B-D), the dispositions of aluminum, iron, and silicon were found at the layer zone adjoining the surface of quartz grain indicated by high concentration of

silicon. They suggest the presence of some kaolinite clay illuviated thinly on the quartz grain, because the ratio of x-ray intensity of aluminum to that of silicon at this layer zone was approximately 2.8:1 (Fig. 1) and this corresponds to that of kaolinite clay. Such distribution of clay and oxides sedimented on the surface of sand grain was revealed with the aid of electron microprobe analyzer.

The elemental analysis by the electron microprobe analyzer are not fully quantitative from several reasons^{2,3}. Firstly, the polishing technique was not efficient enough to give a sufficiently smooth surface, and this is always a problem in case of soil materials. Secondly, no allowance could be made for porosity of the features analyzed. And so

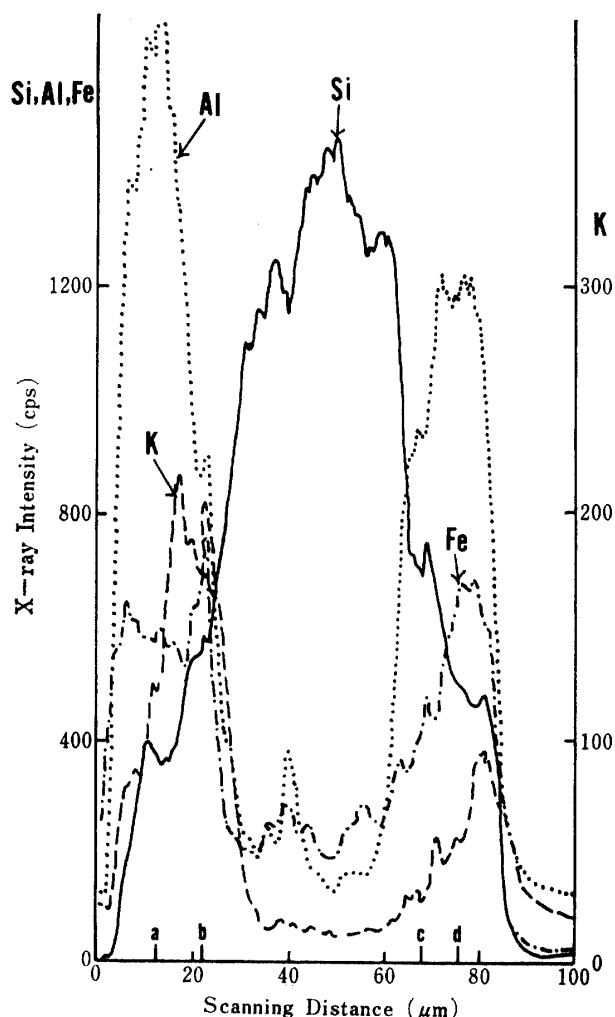


Fig. 2. Elemental distribution at the line (depicted in specimen current picture in Fig. 7) across a specimen of Fig. 7.

only the gross differences have to be discussed in the author's results.

Most of original surface of soil were removed off during the polishing process. Therefore, the sprinkling specimens prepared in the same way as in those for scanning electron microscope were used for the estimation of elemental composition by electron microprobe analyzer. The x-ray intensities of elements obtained in the sprinkling specimen are considered to be a significant, though semiquantitative, information on the elemental distribution of the original surface of soil aggregate.

Micrographs and relating line-graph in Figs. 7 and 2 are results of electron microprobe analyses on unpolished specimen of intact Yamanokami soil. The x-ray images of aluminum, silicon, potassium, and iron in relation to the morphology shown by the specimen current picture in Fig. 7 (A-E) demonstrated that clay encased, as a crust,

the outer surface of sand grain. According to each location of a, b, c, and d in the line scanning analysis as shown in Fig. 2, the relative x-ray intensity of each element within this crust was greatly different. The x-ray image in Fig. 7, (B-E) showed some of spot areas suggesting selectively concentrated element within the crust. One of these spots, about $3 \times 4 \mu\text{m}$ in area at the lower right part was rich in silicon and potassium but virtually contained no iron. The elemental composition of this spot, as determined by the relative x-ray intensity of silicon, aluminum, iron, and potassium, was similar to that of orthoclase used as a reference mineral. Another one of these spots, $4 \times 6 \mu\text{m}$ in area, at the lower left part was likely to be a small skeleton rich in potassium and aluminum and devoid of iron. The rest of spot is considered to be a concentrated iron. Therefore, this crust may be a matrix including various small minerals within the mixture of clay and oxides.

Results of electron microprobe analysis on polished section of Yamanokami soil are given in Fig. 8. This specimen was considered as a matrix principally composed of clay and iron oxide since its current picture was approximately similar to that of distribution of silicon, aluminum, and iron given in area-scanning images. A void, which was $15 \times 20 \mu\text{m}$ in area and occupied with resin, was found in the middle right part. This matrix indicated to include several quartz grains, which were high in x-ray intensity of silicon, though very low in that of other elements, as known by the line scanning analysis (Fig. 3). A circular region, which is about $7.5 \mu\text{m}$ in diameter and shows high x-ray intensity of potassium, in the lower middle part in Fig. 8 (E) appears to be orthoclase from a relative x-ray intensity of silicon: aluminum: potassium (1: 1.2: 0.5). In addition, there were some spots of concentrated iron.

Figure 9 shows the results of scanning electron microscopy and electron microprobe analysis on unpolished specimen of Yamanokami soil. This soil was dispersed by ultrasonic method, air dried, and mounted. The resultant specimen may, therefore, be con-

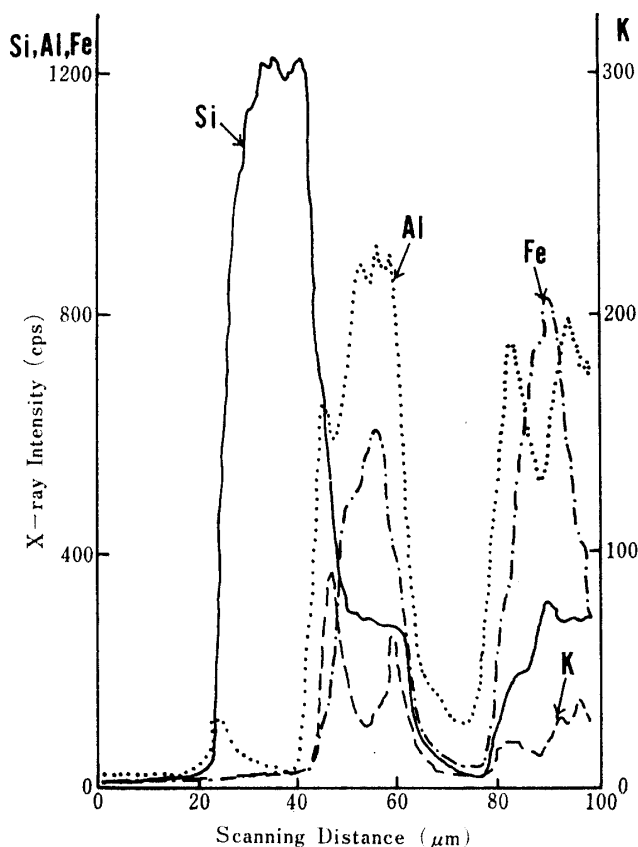


Fig. 3. Elemental distribution at the line (depicted in the x-ray images in Fig. 8) across a specimen of Fig. 8.

sidered as a complex of various minerals reformed during a process of air-drying. It was impossible to distinguish each mineral composing this complex from the picture of secondary electron, but the following consideration will be possible depending upon the x-ray images of silicon, aluminum, iron, calcium, and potassium: 1) The mineral (1 in Fig. 9, B) is assumed to be anorthite according to the relative x-ray intensities of elements at a and b of line scanning analysis (Fig. 4).; 2) The mineral (2 in Fig. 9, B) is judged as quartz because of no element other than silicon.; 3) The mineral (3 in Fig. 9, B) contains silicon, aluminum, iron, and potassium, though iron in its bottom part is somewhat low in concentration compared with that in the remaining part. The elemental composition of this mineral corresponds approximately to that of biotite.

The results of unpolished specimen of intact Kuriyagawa soil are shown in Fig. 10. A rod-shape material of $20 \times 125 \mu\text{m}$ consisted mainly of silicon, and appears morphologically to be some kinds of opal derived from plant residue. Oxides of aluminum and iron are likely to be sedimented separately on the opal-like material, because the relative x-ray intensity of each element varied according

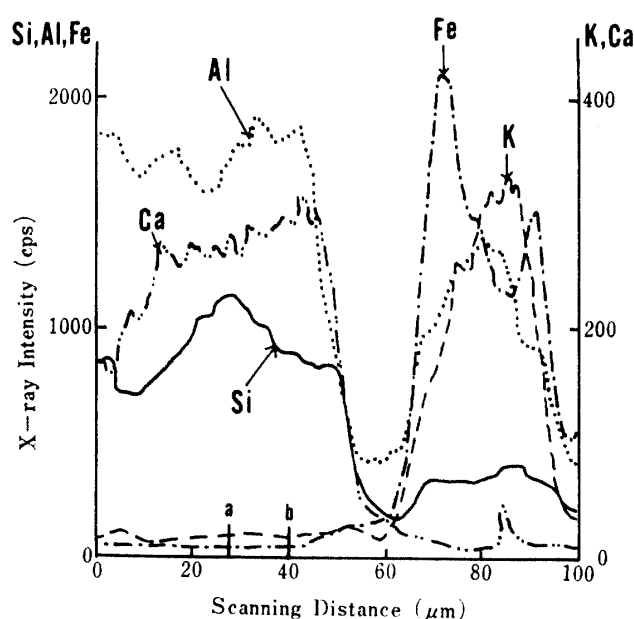


Fig. 4. Elemental distribution at the line (depicted in the x-ray images in Fig. 9) across a specimen of Fig. 9.

to the place of their sedimentation.

The results of microprobe analysis on unpolished specimen of intact Miyakonojyo soil are shown in Fig. 11. It was found clearly in Fig. 11 that the spots of iron lay sporadically on the round soil particle in which silicon and aluminum was codominant. This round soil particle seems to be a quartz grain and it appears to be overlain with a large amount of aluminum oxides as verified by the heterogeneity of x-ray image of aluminum.

The results mentioned above suggest that the application of electron microprobe analysis to the research of soil aggregates will certainly bring us much more detailed informations concerning the distribution of chemically distinct entities within soil aggregates *in situ*. The use of scanning electron microscope together with electron microprobe analyzer seems, therefore, to provide a number of interesting possibilities as regards the interpretation of various aspects of microstructure and formation of soil aggregates.

References

- 1) AZUMA, J. and T. NAKAMURA: *Sci. Rept. Fac. Agr. Kobe Univ.*, **12**, 275-282, 1977.
- 2) BREWER, R., R. PROTZ, and J.A. MCKEAGUE: *Can. J. Soil Sci.*, **53**, 349-361, 1973.
- 3) CESCAS, M. P., E. H. TYNER, and L. J. GRAY: *Advance Agron.*, **20**, 153-198, Academic Press, New York and London, 1968.
- 4) CHILDS, C.W.: *Geoderma*, **13**, 141-152, 1957.
- 5) GALLAHER, R. N., H. F. PERKINS, and D. RADCLIFFE: *Soil Sci. Soc. Amer. Proc.*, **36**, 181-183, 1972.
- 6) GALLAHER, R. N., H. F. PERKINS, and D. RADCLIFFE: *Ibid.*, **37**, 465-469, 1973.
- 7) GALLAHER, R. N., H. F. PERKINS, K. H. TAN, and D. RADCLIFFE: *Ibid.*, **37**, 469-472, 1973.
- 8) HILL, D. E. and B. L. SAWHNEY: *Soil Sci.*, **112**, 32-38, 1971.
- 9) MURAKAMI, S.: *Seibutsugaku Jikkenho Koza* (in Japanese) (*Course on Experimental Method of Biology*), Supplement 2, 1st Ed., 39-85, Nakayama Shoten, Tokyo, 1969.
- 10) SAWHNEY, B. L.: *Soil Sci. Soc. Amer. Proc.*, **37**, 658-660, 1973.
- 11) Shimadzu Seisakusho: *X-sen Maikuro Anaraiza ni yo ru Bunsekiho to Shiriyo Sakusei* (in Japanese) (*Analytical Method by X-ray Micro-analyzer*

- and Preparation of Sample), Shimadzu Seisakusho Ltd., Kyoto, 1973.
- 12) SOMASIRI, S. and P.M. HUANG: *Soil Sci. Soc. Amer. Proc.*, **37**, 461-464, 1973.
- 13) UCHIYAMA, I., A. WATANABE, and S. KIMOTO: *X-sen Maikuro Anaraiza* (in Japanese) (*X-ray Microanalyzer*), 5th Eds. Nikkan Kogyo Shinbun Ltd., Tokyo, 1974.

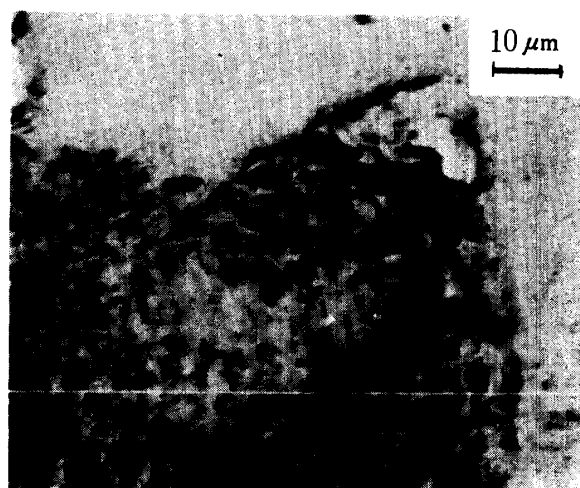
土壌集合体を構成する鉱物に関するX線マイクロアナライザ分析

東 順 三・中 村 俊 博・石 沢 修 一

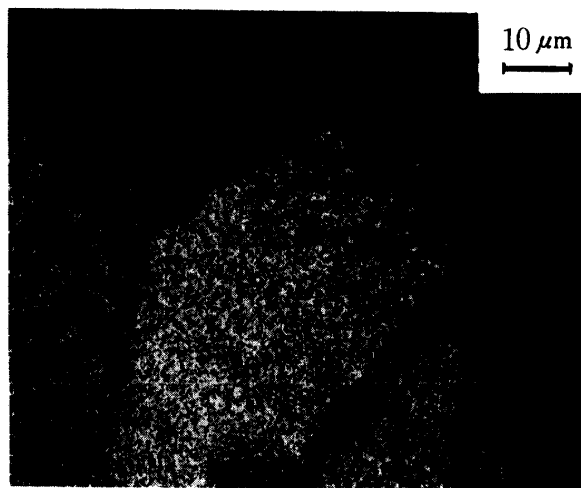
要 約

火山灰と非火山灰に由来するそれぞれ2種の土壌を、そのまま試料台にふりかけた試料と樹脂包埋後研磨した切片試料についてX線マイクロアナライザで元素分析した。得られた土壌集合体の微細域の主要元素分布の差異に基づいて次のものの様相を認知することができた。

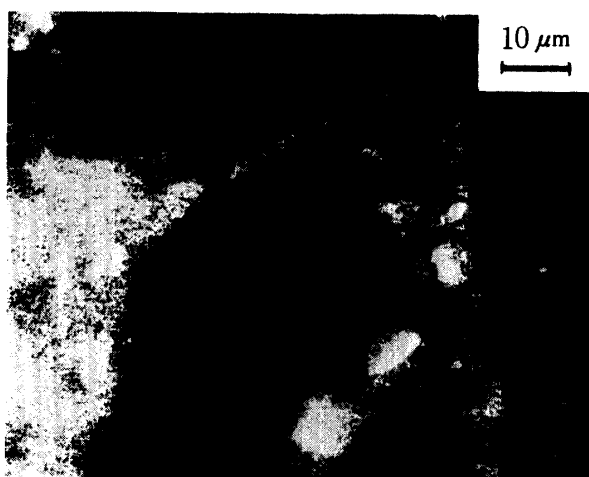
1. 異種鉱物の集合によって形成されている土壌集合体。
2. 石英粒の表層に沈積した粘土と鉄・アルミニウムの酸化物。
3. 粘土を主体とするプラズマ基質中に包含された骨格粒子と空隙。
4. 砂粒上に散在する斑鉄。
5. 土粒間および粒団間で接着物質の役割を演じている粘土と鉄・アルミニウムの酸化物。



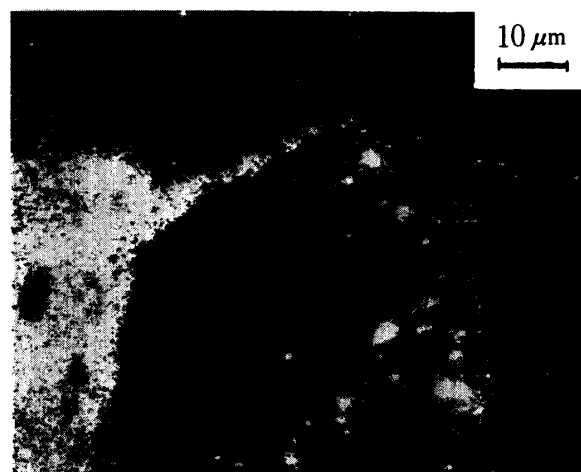
(A) Specimen current picture



(B) Si x-ray image

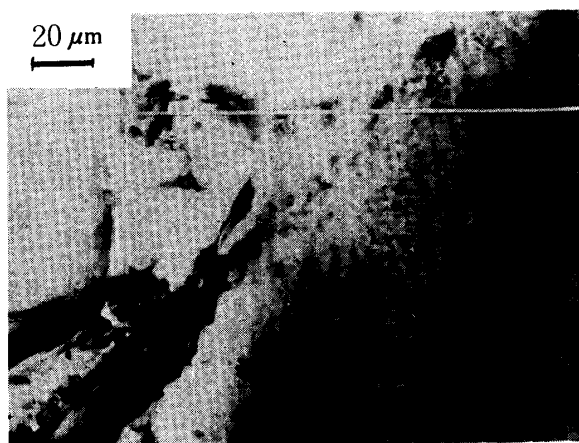


(C) Al x-ray image

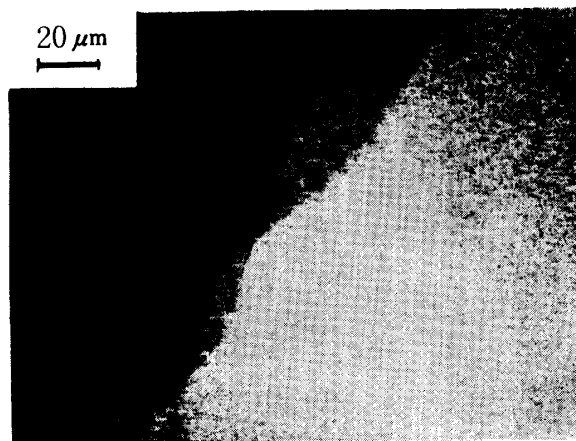


(D) Fe x-ray image

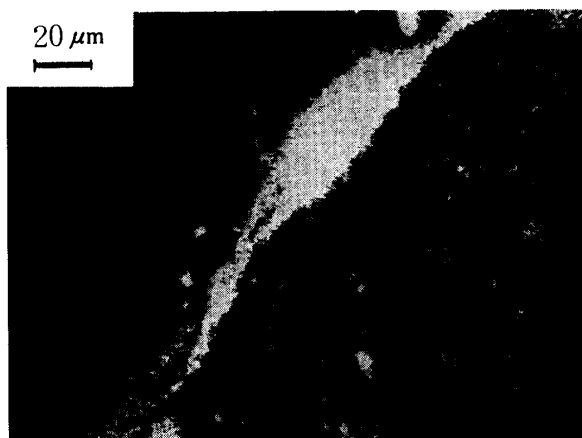
Fig. 5. Specimen current picture and congruent x-ray images of Si, Al, and Fe illustrating quartz grains connected with iron oxide and kaolinite clay. (polished section specimen of synthetic aggregate prepared in laboratory).



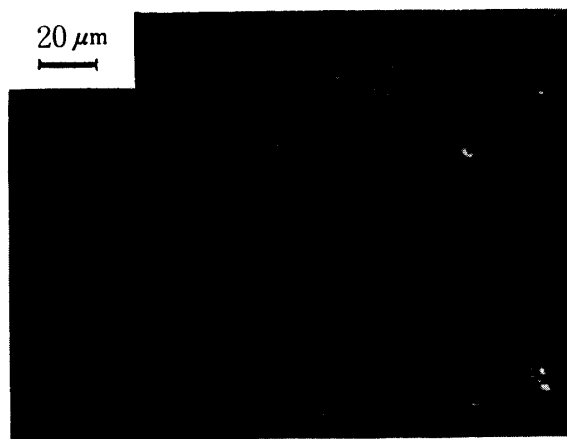
(A) Specimen current picture



(B) Si x-ray image

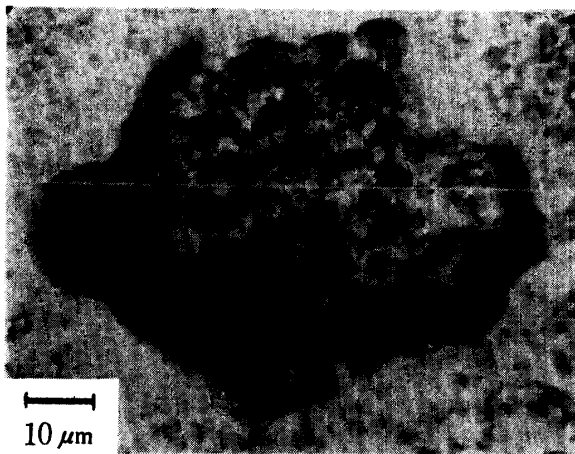


(C) Al x-ray image

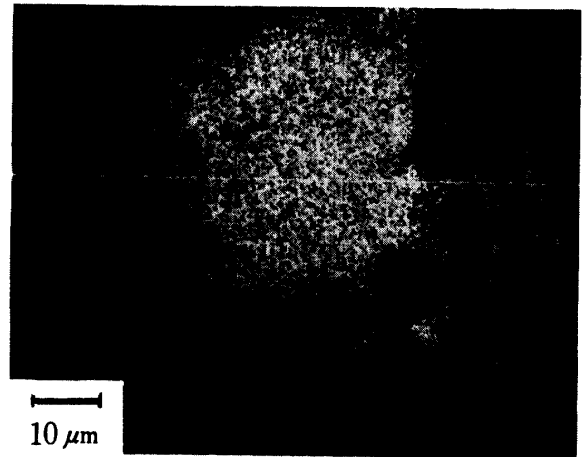


(D) Fe x-ray image

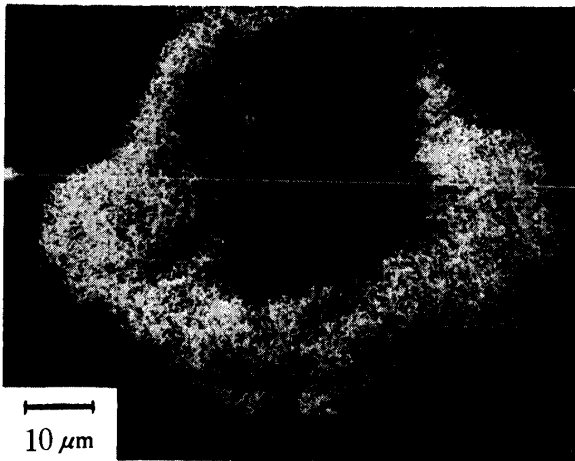
Fig. 6. Specimen current picture and congruent x-ray images of Si, Al, and Fe showing a surface of sand grain having clay and iron oxide. (polished section specimen of Higashishiroyama soil, Hyogo prefecture).



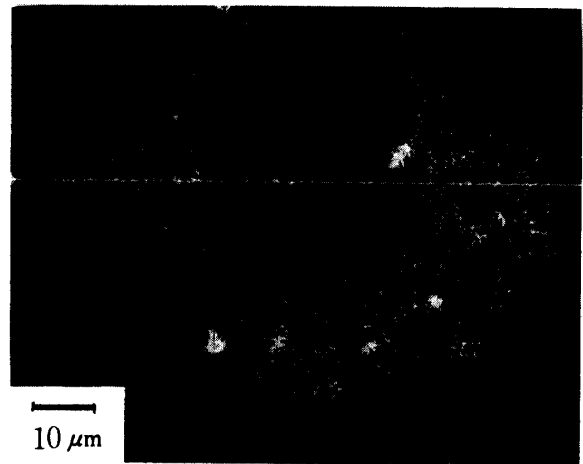
(A) Specimen current picture



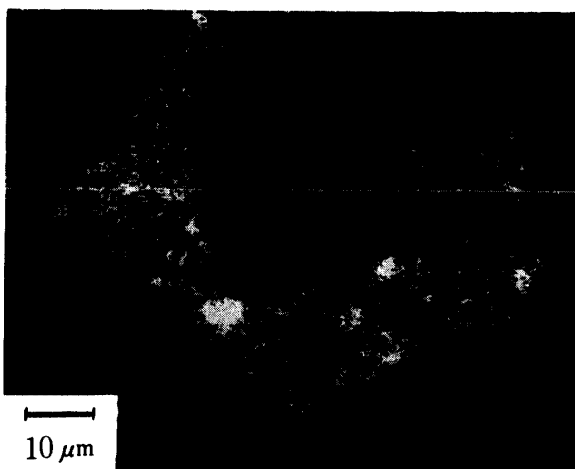
(B) Si x-ray image



(C) Al x-ray image

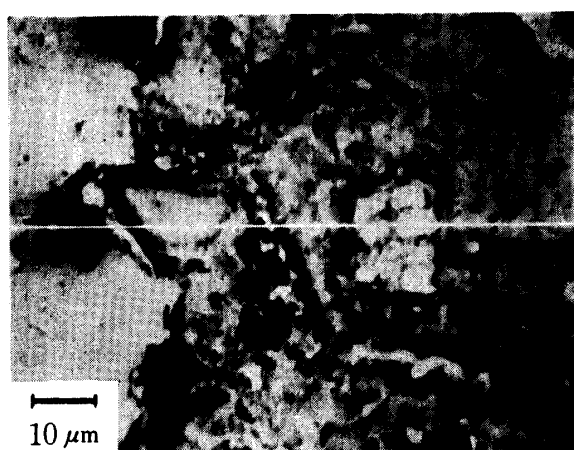


(D) Fe x-ray image

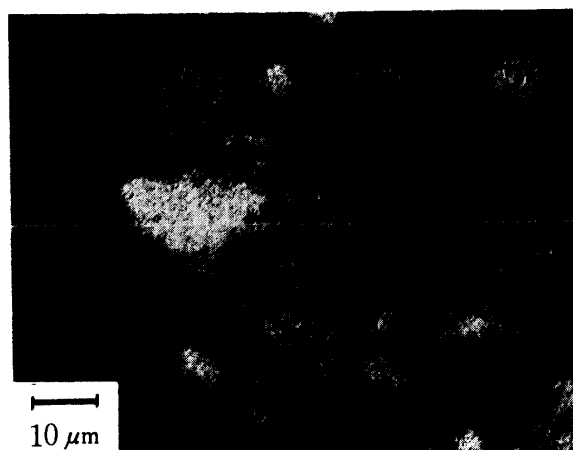


(E) K x-ray image

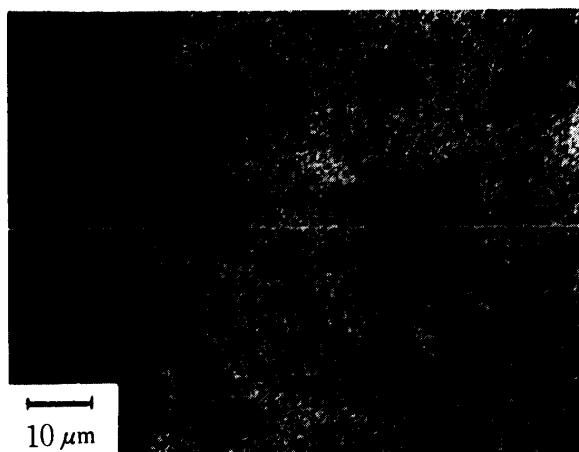
Fig. 7. Specimen current picture and congruent x-ray images of Si, Al, Fe, and K illustrating a sand grain encased with clay as a crust. (unpolished sprinkling specimen of Yamanokami soil, Hyogo prefecture.)



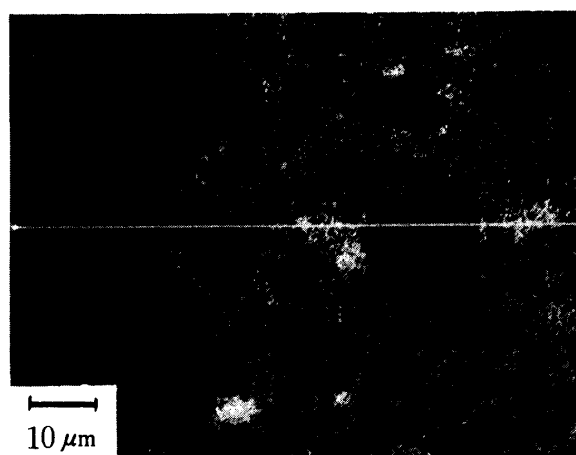
(A) Specimen current picture



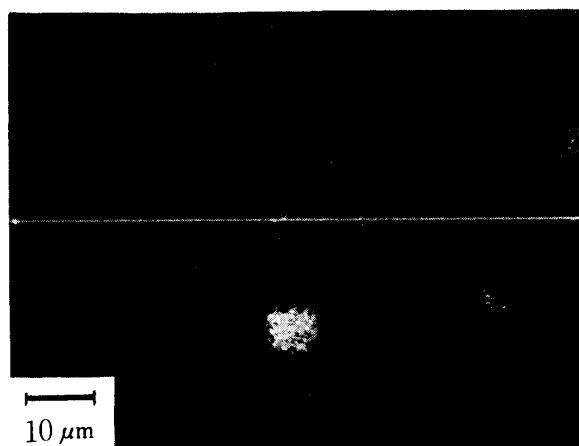
(B) Si x-ray image



(C) Al x-ray image

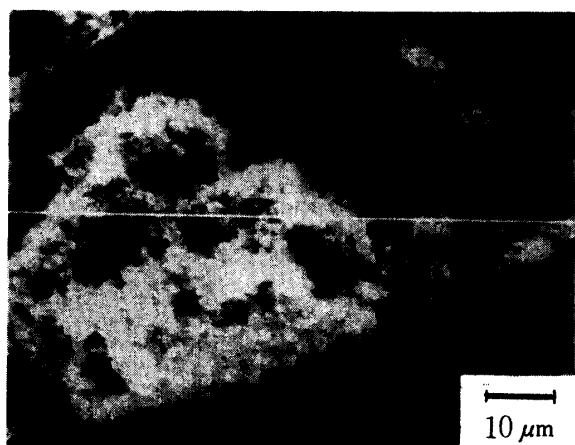


(D) Fe x-ray image

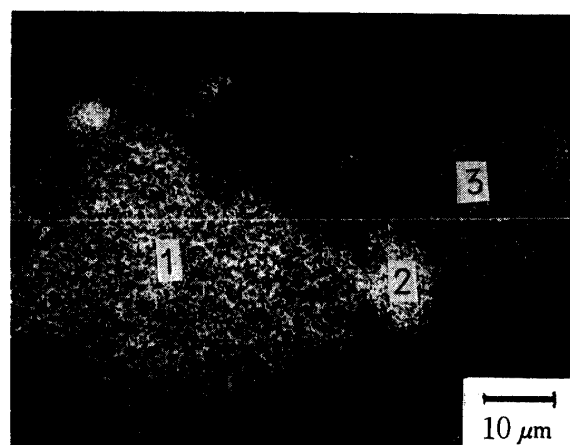


(E) K x-ray image

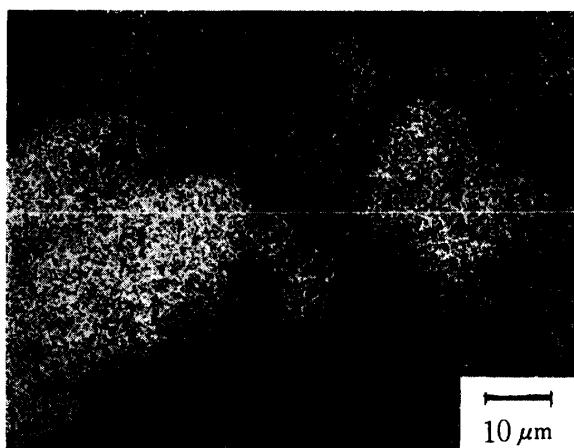
Fig. 8. Specimen current picture and congruent x-ray images of Si, Al, Fe, and K showing a skeleton inclusion and a void within a matrix. (polished section specimen of Yamanokami soil, Hyogo prefecture).



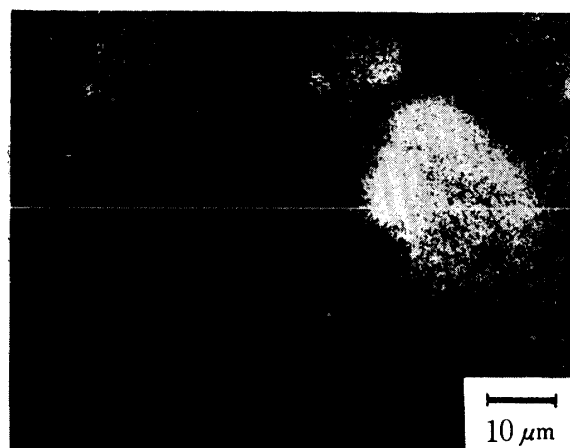
(A) Secondary electron picture



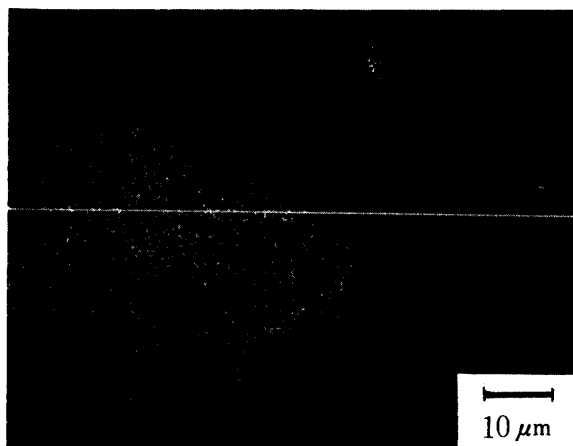
(B) Si x-ray image



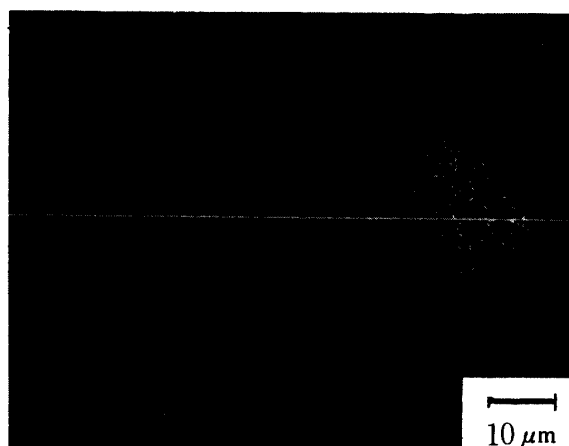
(C) Al x-ray image



(D) Fe x-ray image

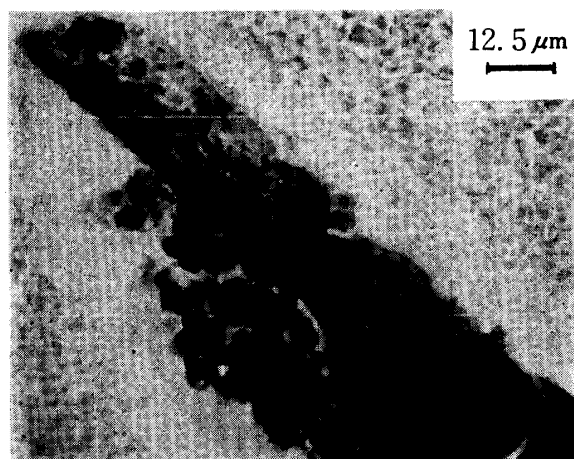


(E) Ca x-ray image

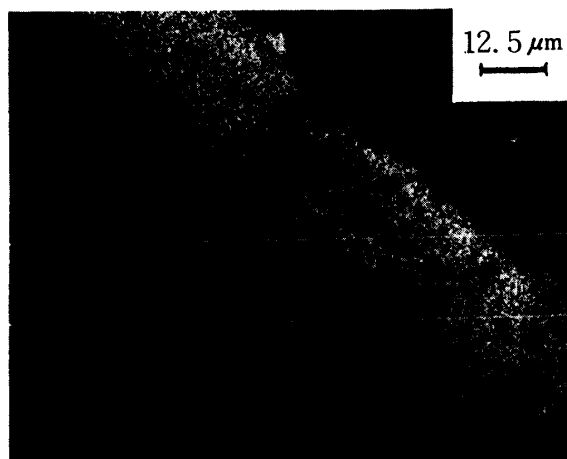


(F) K x-ray image

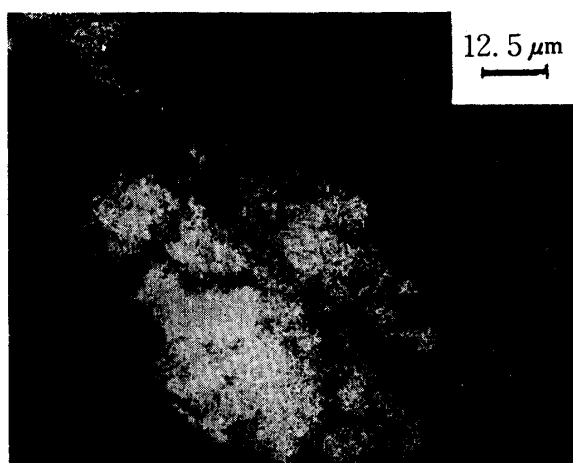
Fig. 9. Secondary electron picture and congruent x-ray images of Si, Al, Fe, Ca, and K illustrating a resynthesized soil composed of several different minerals. (unpolished sprinkling specimen of Yamanokami soil, Hyogo prefecture).



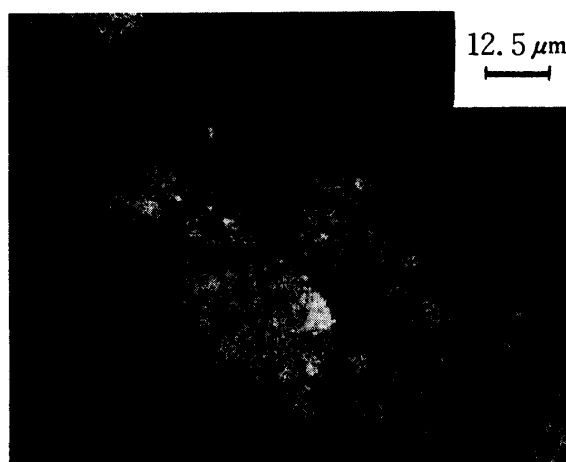
(A) Specimen current picture



(B) Si x-ray image

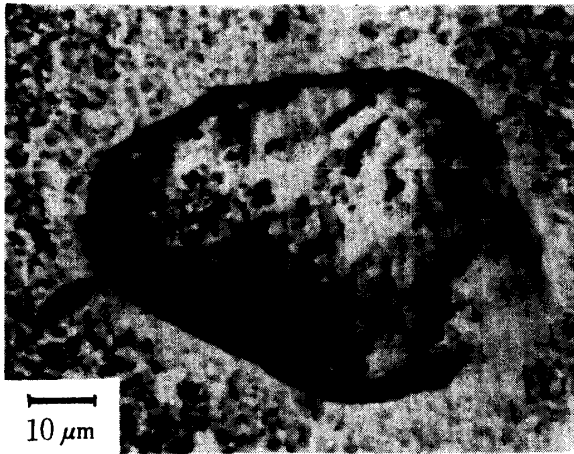


(C) Al x-ray image

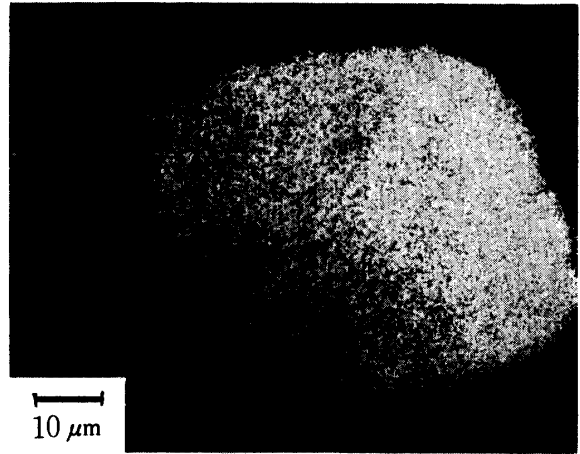


(D) Fe x-ray image

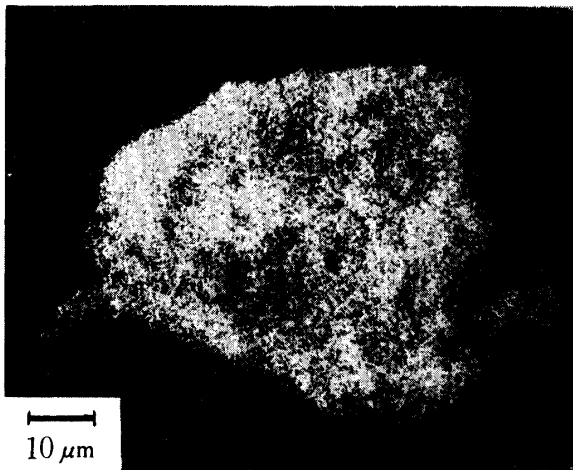
Fig. 10. Specimen current picture and congruent x-ray images of Si, Al, and Fe showing oxides sedimented locally on the opal-like material of plant origin (unpolished sprinkling specimen of Kuriyagawa volcanic ash soil, Iwate prefecture).



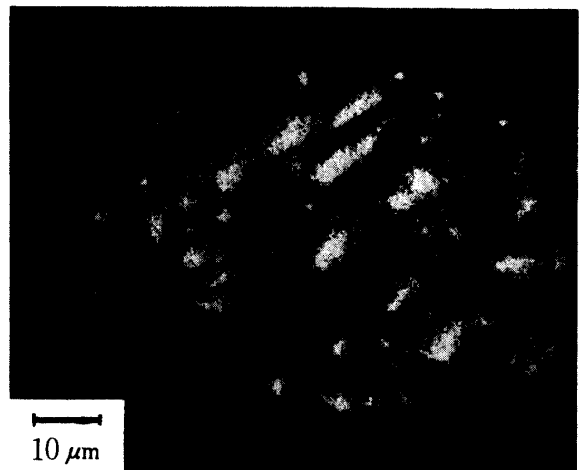
(A) Specimen current picture



(B) Si x-ray image



(C) Al x-ray image



(D) Fe x-ray image

Fig. 11. Specimen current picture and congruent x-ray images of Si, Al, and Fe showing mottled irons on a sand grain. (unpolished sprinkling specimen of Miyakonojyo volcanic ash soil, Miyazaki prefecture).